V European Conference on Computational Fluid Dynamics
ECCOMAS CFD 2010
J. C. F. Pereira and A. Sequeira (Eds)
Lisbon, Portugal,14-17 June 2010

INVESTIGATIONS OF IGNITION PROBABILITY OF A FORCED IGNITED TURBULENT METHANE JET USING LES

J. Weckering*, A. Sadiki†, J. Janicka† and E. Mastorakos††

*,†Institute Energy and Powerplant Technology, TU Darmstadt
Petersenstr. 30, 64287 Darmstadt, Germany
e-mail: weckering@ekt.tu-darmstadt.de
††Hopkinson Laboratory, Department of Engineering, University of Cambridge

Key words: Large Eddy Simulations (LES), time-resolved Lagrangian particles monitoring, forced ignition

Abstract. *This paper presents a LES-based methodology based on statistical analysis of flow, mixing, turbulent flame speed and ignition events, for predicting the probability of igniting a turbulent non-premixed jet flame with a localized spark. In the context of forced ignition of turbulent non-premixed mixtures the transition from a non burned state to a stable burning regime strongly depends on turbulence and mixture inhomogeneity effects [1, 2]. Besides, ignition is a transient phenomenon that strongly interacts with the turbulent flow. As a consequence, the time resolved calculation of an ignition sequence (as simulated by Lacaze et al. [3]) requires high computational ressources, to such an extent that this method is difficult for performing statistical analysis. Though, the statistical analysis of the stationary jet delivers precious information in terms of probability of successful flame kernel generation and of flame front blow-out stability. The proposed method allows performing statistical analysis based on ensemble averaging, and this at a low computational cost. The results of numerical investigations of a spark ignited turbulent methane jet are presented and compared to experimental investigations by Ahmed et al. [2]. In particular, the probability of successful flame kernel, the local flame speed, the subsequent region of possible upstream flame propagation and the convection of flame kernels as well as the probability of upstream flames propagation have been pointed out.*

1 INTRODUCTION

Ensuring successful ignition of practical combustion applications is a challenging issue in the design process of new combustion systems. The development of lean burn concepts in aero-engine combustors for reducing the formation of thermal nitrogen oxides is accompanied by less stabile combustion conditions, which also impact on the ignition processes leading to a full relight of the combustor. Thus, the development of advanced low-NOx aero-engines is impeded by the necessity of ensuring an effective relight for all operating conditions. In particular, the relight capability at high altitudes is a key issue and there is a strong interest from the aero-engines manufacturers for numerical methods capable of predicting the ignition processes involved in the effective relight of gas turbines.

Four stages are basically identified in the successful relight of a gas turbine: (i) energy deposition, (ii) formation of a viable flame kernel, (iii) flame growth and propagation and (iv) stabilization. The present study focuses on part (iii) in gaseous mixtures. In non-premixed turbulent flows the fluctuations of the mixture fraction at ignition location result in a probabilistic behavior of the generation of a kernel of flame following energy deposition [1, 2]. Birch et al. [4] and Smith et al. [5] investigated this behavior. In turbulent non-premixed jet flames, they measured the probability of finding a flammable mixture, called flammability factor, P_F, as well as the probability of generating a sustainable kernel, P_{ker}. They found that the region of stochastical flammability ($P_F > 0$) is wider than the zone where the mean mixture fraction has flammable values and that the probability of generating of kernel of flame is similar to the flammability factor on the jet axis ($P_{ker} \approx P_F$).

Detailed information on ignition probability and transient behavior of ignited kernels has been provided by Ahmed et al. for different gaseous non-premixed turbulent configurations, such as jets [2], counterflows [6] and recirculating flames [7]. Regarding the jet configuration, they showed that the stabilization and upstream propagation of a flame following ignition occur in a tubular region of flammable mixture and low velocity flow. They also demonstrated the existence of regions which are favorable to flame kernel initiation (P_{ker} high), but where the generated kernels frequently fail to propagate to the tubular stabilizing region, so that the flame can not stabilize and the kernel is blown out (P_{ign} low). Hence, the ignition stage consisting of the transition from a stratified charge kernel to a stratified or partially premixed upstream propagating flame is a key process in a successful ignition sequence. The dynamics of this ignition process depends on the scales of time-dependent turbulent motion. Thus, methods that are spatially and time-resolved like large eddy simulations (LES) are required. A comprehensive review on reactive LES can be found in [8].

Using LES, time-resolved calculations of ignition sequences have been performed in [3, 9, 10, 11, 12]. However, the prediction of experimentally-observable ignition probability maps requires ensemble averaging of numerous time-resolved events. Given the high computational costs of the existing single event simulations, such methods are excluded

for performing statistical analysis.

Nonetheless, the transient behavior of a flame kernel is mainly determined by large scale flow structures, that are present in the turbulent flow field at ignition time. Hence, the blow-out of successful generated flame kernels, as observed in [2], may be determined from the analysis of the turbulent flow field of the stationary jet at ignition time.

Hence, this paper proposes a methodology for investigating the possible stabilization of convected flame kernels based on (i) the time-resolved calculation of the stationary jet, on (ii) the monitoring of convected computational particles that are representative for ignition events, (iii) on the experimental observations of the kernel growth and (iv) on the local turbulent flame velocity. A conceptually similar effort, aimed to predict whole-flame ignition probability by considering the motion of virtual flame elements in a flow field provided by an inert RANS solution, has been attempted by Richardson [13] with good results as compared to experiment.

To demonstrate the validity of the method, this will be applied to spark ignition of a turbulent methane jet in ambient air. Section 2 provides an outline of the configuration. The modeling and numerical approaches are given in section 3. Section 4 presents the numerical results and related discussions. Section 5 is devoted to conclusions.

2 CONFIGURATION

The configuration under study consists of a turbulent methane-air jet experimentally investigated in [2] and simulated in [3]. A 5 mm diameter (d) jet of fuel (70% of methane and 30% of air by volume) with a bulk velocity of 12.5 m/s issues into a 200 mm diameter co-flow of air moving at $Uc = 0.1$ m/s. The Reynolds number of the jet is $Re_j = 2878$. The jet extends to 130 d downstream of the nozzle so that the internal flow is expected to exhibit a fully developed turbulent velocity profile. The authors measured at first step the mean and fluctuating velocity components for a pure air jet. A pair of electrodes was positioned at various locations throughout the flow. A spark with an overall duration of 400 μs and a nominal electrical energy of 100 mJ with an electrode spacing of 1 mm and tip diameters of 0.1 mm was then used.

Following the spark, three main stages for the ignition and the subsequent flame propagation have been observed in [2] and in [3] for a 25 m/s jet: i) radial flame kernel size linearly growing with time, ii) downstream flame propagation and radial expansion; and finally iii) tubular upstream flame propagation, see Fig. 1(a) and (b). All the experimental results are reported in detail in [2]. Figures 1(c) and (d) illustrate the modeling strategy for investigating the probability of flame stabilization after 10 ms. This modeling is presented in detail in section 4.3.

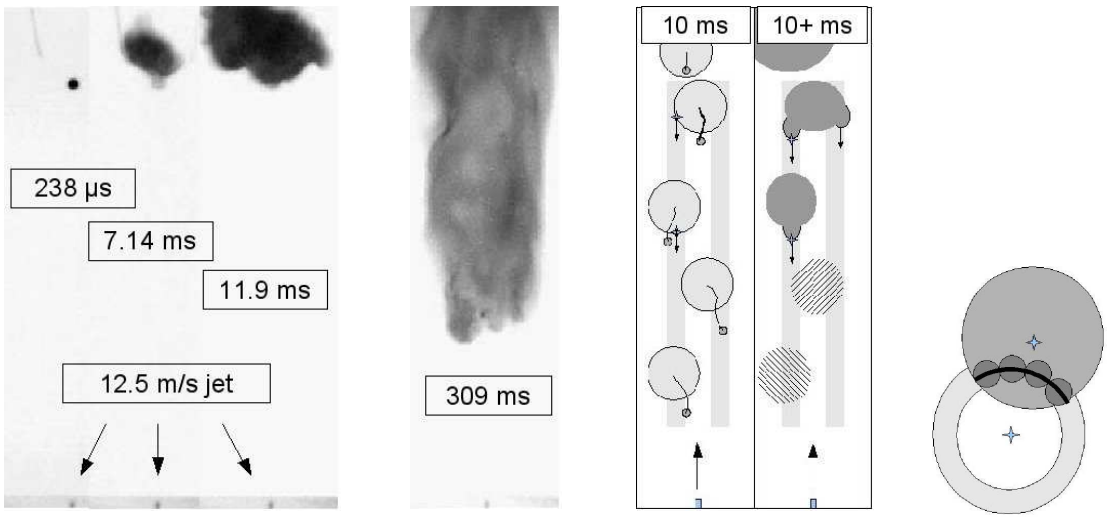

(a) (b) (c) (d)

Figure 1: (a) High speed camera images of an ignition sequence from the flame kernel generation to the transition to an upstream propagating flame ($238\ \mu s; 7.14\ ms; 11.9\ ms$) in [2]. (b) Tubular upstream propagating flame at 309 ms in [2]. (c) Schematics of the simultaneous monitoring of Lagrangian particles representative for ignition events, showing five simultaneous events in the flammable zone, at two time steps: 10 ms (left) and a few ms later (right). Surfaces show two quenching events due to high strain (dashed), two successful transitions to upstream propagating flames in the tubular zone and one kernel blow-out event. (d) Schematic of the contact surface between the flame kernel (dark grey) and the tubular zone (fair grey), showing four conceptually independent locations distant of maximal anti-correlation distance, 1 d, from each other.

3 MODELING APPROACH AND NUMERICAL SET-UP

3.1 LES

In LES, the larger scales are directly resolved, while the smaller scales are modelled. The Favre-filtered continuity (1), momentum (2) and scalar transport (3) equations read:

$$\frac{\partial \overline{\rho}}{\partial t} + \frac{\partial (\overline{\rho} \widetilde{u}_i)}{\partial x_i} = 0, \tag{1}$$

$$\frac{\partial \overline{\rho} \widetilde{u}_i}{\partial t} + \frac{\partial \overline{\rho} \widetilde{u_i} \widetilde{u_j}}{\partial x_j} = -\frac{\partial \overline{p}}{\partial x_i} + \frac{\partial \widetilde{\tau_{ij}}}{\partial x_j} + \frac{\partial \left(\overline{\rho} \tau_{ij}^r \right)}{\partial x_j}, \tag{2}$$

$$\frac{\partial \overline{\rho} \widetilde{Y}}{\partial t} + \frac{\partial \overline{\rho} \widetilde{u_i} \widetilde{Y}}{\partial x_i} = \frac{\partial}{\partial x_i} \overline{\rho} \left[\widetilde{D} \left(\frac{\partial \widetilde{Y}}{\partial x_i} \right) - J_i^{SGS} \right]. \tag{3}$$

A simple Smagorinsky model is employed to close the sub-grid scale (SGS) stress-tensor, τ_{ij}^r, with Lilly's formulation of Germano's dynamic procedure for the model coefficient [14].

In the filtered scalar equation, the diffusion coefficient is linked to viscosity via the Schmidt number for which a value $Sc = 0.7$ is assumed. This relates to gaseous mixing. An eddy diffusivity model is used for the SGS scalar flux, assuming a constant Schmidt number relationship between the turbulent diffusion coefficient and the turbulent viscosity, $Sc_t = 0.7$. The SGS kinetic energy, k_Δ, was calculated from the turbulent viscosity, using Eq. (4), with $C_{yo} = 0.086$ according to [15]. The SGS velocity fluctuation, v'_Δ, is given by Eq. (5).

$$k_\Delta = {\nu_T}^2/(C_{yo}\Delta)^2 \tag{4}$$

$$v'_\Delta = \sqrt{2k_\Delta/3} \tag{5}$$

All the governing equations are integrated into the three-dimensional finite-volume unstructured CFD code PRECISE-UNS, developed in cooperation with Rolls-Royce. Second-order central schemes are used for spatial discretization except for the convection term in the scalar transport equation. Here a flux-limiter with total variation diminishing properties is employed to ensure bounded solutions for mixture fractions. Pressure-velocity coupling is achieved via a SIMPLE similar procedure extended for low-Mach number flows. As time integration a second order implicit three time level method is used.

3.2 Simultaneous monitoring of multiple ignition events

The convection of flame kernels is retrieved by monitoring fluid particles representative for ignition events. The particles are seeded in the stationary inert flow and are tracked by a Lagrangian method. The effects of thermal expansion due to the generation and growth of flame kernels on the turbulent flow are not directly simulated. Although thermal expansion impacts on the turbulent flow, the probabilistic convection of a kernel is considered as being mainly determined by large scale structures that are already present in the non-ignited flow at ignition time. Thus, an adequate analysis of the stationary inert flow should allow to investigate the probabilistic convection of ignited kernels.

According to observations in [2], the transition from a radially expanding kernel to a propagating flame capable of upstream displacement in case of successful ignition takes about 10 ms. During the first milliseconds following spark, the mixture conditions over the surface of kernel can be considered as homogeneous, due to the small size of the kernel in the stratified mixture. Hence, the growth of the kernel during the first milliseconds results in an isotropic thermal expansion. The isotropic effect of thermal expansion is considered as not affecting the convection of the kernel centers. Thus, the center of a flame kernel is expected to follow the same movement as the corresponding fluid element would have follow in the non-ignited configuration. Therefore, the particles representative for ignition events are considered as they exactly follow the turbulent flow. The kernel deformation due to heterogeneous flow conditions over the radially growing kernel are not considered in the modeling.

Hence, the monitoring of an ignition event is performed by tracking a Lagrangian particle within the LES of the stationary turbulent jet. Since the monitoring of an ignition event does not affect the stationary flow, it is possible to monitor simultaneously multiple ignition events, that are originated at different locations and different instants. Finally, the monitoring of multiple ignition events allows to perform a statistical analysis of the convection of flame kernels based on ensemble averaging at a low computational cost. Indeed, the computational cost for performing this ensemble averaging is expected to scale with the computational cost required for performing a statistical analysis of the stationary configuration based on LES.

Moreover, the monitoring of flow properties encountered by spatially distributed particles allows to analyse the statistical conditions within the flow. On the large-eddy scale, the turbulent flame brush can be represented as a thick front propagating at speed $s_{\widehat{T}}$. In the context of premixed mixtures, correlations have been investigated to evaluate the turbulent flame speed, see [16, 17, 18]. Here, $s_{\widehat{T}}$, is determined at the LES filter size, using the sub-grid velocity fluctuations, as applied in [17], Eq. 6:

$$s_{\widehat{T}}/s_L = 1 + C\,(v'_\Delta/s_L)\,. \tag{6}$$

Although this model is basically devoted to premixed flames, the method is expected to provide satisfying estimation of the turbulent flame speed in stratified-charge and partially premixed mixtures with high premixing level. A further restriction to the turbulent speed modeling regards the constant, C, which depends on the estimation of the sub-grid turbulent kinetic energy. Even though, C, can be adjusted through a dynamic procedure as in [17], the uncertainties implied by mixture stratification effects, would potentially annihilate the benefits of the dynamical approach. Hence, C is considered as constant here. The determination of its level is discussed in Section 4.2.

To evaluate s_L, a 1-dimensional laminar flame code based on detailed chemistry is applied. Here the chem1d code from the Technical University Eindhoven is used with GRI-3.0 mechanism for methane from Berkeley University [20].

A parabolic fitting function according to the method by Metghalchi and Keck [19] allows to determine the local laminar flame speed, s_L, during calculation. Finally, a field of axial flame net displacement speed is calculated by subtraction of the resolved axial flow velocity.

3.3 Numerical set-up

A block-structured mesh has been used and optimized for the simulation of ignition events. The total number of cells is 1.5×10^6. The minimal cell at jet outlet is $0.3 \times 0.3 \times 0.15\ mm^3$ while it is of $1.4 \times 0.65 \times 0.65\ mm^3$ on the jet axis at 50 d.

As inlet boundary conditions, a turbulent pipe flow is generated over a distance of 10 d. No special measures are taken to impose artificial turbulence on the inflow. For the co-flow, an inflow distance of 20 d is calculated.

Two cases for which experimental results are available have been investigated. The first features an air-air jet mixture with a bulk velocity of 21 m/s. It is used to appraise the LES methodology. The second case consists of the methane-air jet described in section 2. This is chosen for model validation.

With respect to the Lagrangian particles tracking, a total amount of about 55,000 statistically independent particles are injected into the ignitable region of the non-ignited turbulent flow. Each particle is representative of an ignition event and their history is monitored over 20 ms. The possibility of upstream flame displacement is evaluated over the kernel surface. Therefore, a kernel diameter of 35 mm at 10 ms is considered, based on the visualization of [2]. The modeling applied for deriving the probability of finding an upstream axial net velocity over the kernel surface is detailed in section 4.3.

4 RESULTS AND DISCUSSION

4.1 Mixing field

Fig. 2 (left) shows the radial distribution of the mean axial velocity, U, scaled by the respective values on the axis, U_m, for the air/air jet. Fig. 2 (right) displays the radial distribution of the axial velocity fluctuation, U'. Typical jet self-similarity characteristics are obtained, as well as good agreement with the experimental data [2]. This allowed to demonstrate the prediction capability of the LES methodology, that was then used for further investigations.

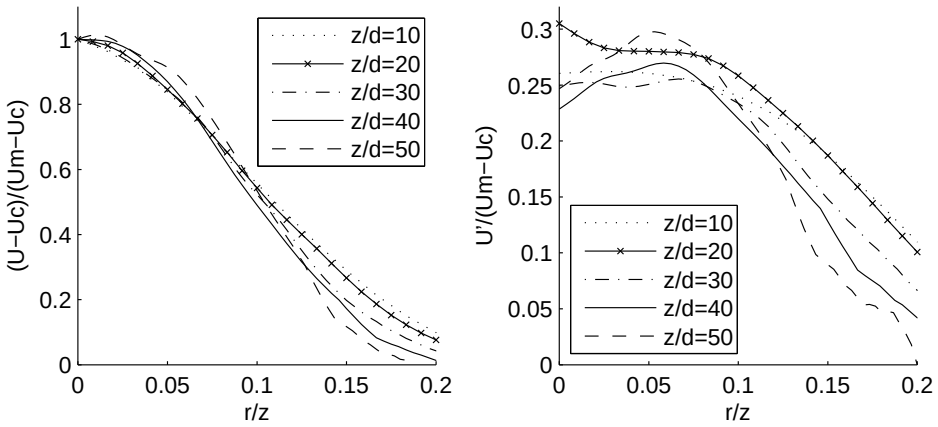

Figure 2: Radial distribution of the mean axial velocity (left), and of its fluctuation (right). 21 m/s air jet

Figure 3(a) shows how the LES allows to predict the mixing field of the methane-air jet. Thereby, the correlation by Richards and Pitts [21] is applied to provide an estimation of the mean mixture fraction as a function of the axial position, z, and of a non-dimensional

radial coordinate, $\theta = \frac{r}{z-7.2\ r_{jet}}$:

$$\bar{f}(z,\theta) = \left(\frac{\rho_{jet}}{\rho_{air}}\right)^{1/2} \frac{9.52\ r_{jet}}{z - 7.2\ r_{jet}} exp\left(-59\ \theta^2\right). \tag{7}$$

Figure 3(b) displays the probability of finding a flammable mixture called flammability factor, P_F. It is representative of the probability of generating a viable flame kernel, P_{ker}, in regions of moderate strain, which can be found in the downstream region ($z > 30\ d$) and are in the focus of the present study. This was calculated by time-integration of the realization of mixture fraction between the lean and rich flammability limits.

4.2 Flame stabilization region

According to observations in [2], the transition from a radially expanding kernel to a propagating flame capable of upstream displacement in case of successful ignition takes about 10 ms. This is the time required until the kernel reaches a width of about 7 d. At that time, the kernel surface reaches a flame stabilizing region characterized by near-stoichiometric mixture and low velocity flow.

Figure 3(c) shows a scatter plot of the upstream flame speed on the axial direction, restricted to particles with radial positions between 2 and 4 d, at 4 time steps (0, 5, 10, 15 ms) of a 15 ms sequence, as well as the measured upstream speed [2]. The majority of the particles display negative values (i.e. would be convected downstream). However, flame wrinkling increases the flame propagation velocity and the overall upstream flame speed can be assessed from the particles with the highest velocities representative of the velocity of the leading part of the flame surface. Indeed, visualization of ignition events shows a "tongue-like" upstream propagation, with significant variations in the shape of the leading edge of the flame [2, 6, 7], which is consistent with the view that only few particles can be responsible for overall successful upstream flame ignition.

The comparison to the experimental upstream speed provide a method to adjust the constant C, in Eq. 6, accounting for SGS flame wrinkling effects. Hence, a coefficient value of, $C = 2.5$, close to the value of 2.25 used in [16], is found to deliver maximum upstream speed consistent with experimental data.

A contour plot of upstream flame speed was generated considering only particles with upstream velocities, ($U_{up} > 0$). The flame stabilizing region, Fig. 3(d), displays a tubular form with radial positions between 2 and 4 d. This agrees well with the observation of a tubular upstream flame propagation, see Fig. 1(b). The level of the upstream speed is also in good agreement with the experimental data.

4.3 Probability of upstream flame displacement

Considering the form of the stabilizing region and the upstream flame speed distribution in this region it is possible to evaluate the probability of upstream flame displacement at any point. Outside the tubular stabilizing region the probability is found to be zero.

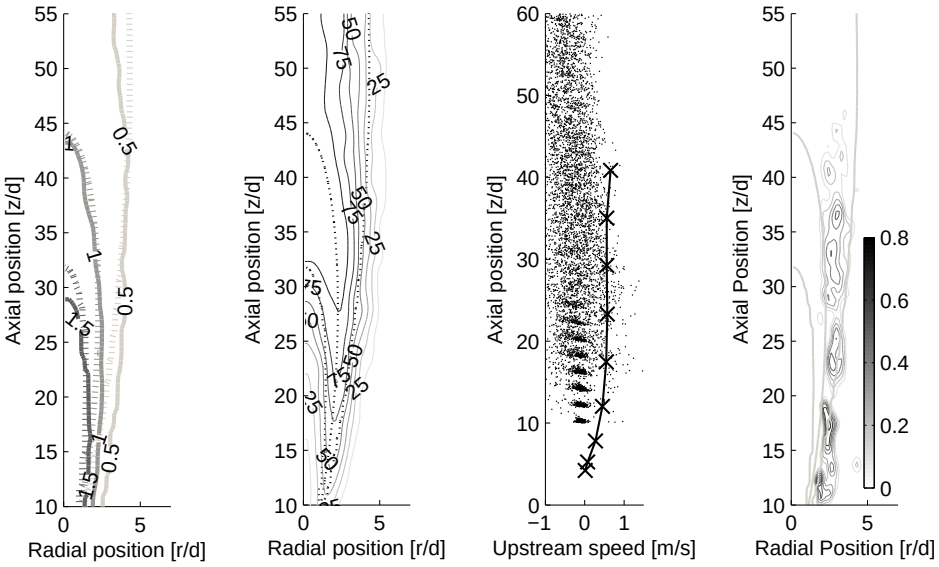

(a) (b) (c) (d)

Figure 3: (a) Mean mixture fraction fields after Richards' correlation [21] (dashed) and from LES. Isolines show equivalence ratio of 0.5, 1. and 1.5. (b) Flammability factor representative of the probability of successful kernel generation, P_{ker}. (c) Scatter plot of upstream flame speed and measured absolute flame speed in [2]. (d) Field of upstream flame speed [m/s], conditioned on particles with positive speed.

Within the region, the probability is evaluated from the fraction of points with an upstream flame speed for a given axial position $P_1(z)$, which is derived from the scatter plot displayed on Fig. 3(c).

The dashed line on Fig. 4 shows the probability of upstream flame displacement inside the stabilizing region over axial position for a single point. A maximal probability close to 30% is reached within a range of axial positions between 28 and 35 d, where low flow velocities and near-stoichiometric mixture fractions are favorable for stabilization. Further downstream, increased mixing with the coflow results in leaner mixtures and lower flame speeds, so that the probability of upstream flame displacement decreases continuously and becomes zero at an axial position of 60 d.

The probability of upstream flame displacement needs to be integrated over the surface of a flame kernel. This probability, $P_{up}(z, r_{ker})$, is expressed in Eq. 8, as a function of the axial position z and of a conceptual number, n_{surf}, of statistically independent locations on the contact surface between the kernel and the tubular region.

$$[1 - P_{up}(z, r_{ker})] = [1 - P_1(z)]^{n_{surf}} \tag{8}$$

On the jet axis, the surface of the kernel is in contact with the whole surface of the stabilizing ring. Based on the distance of maximal anti-correlation, a maximal number of $n_{surf} = 7\pi \approx 22$ is applied for integrating the probability over the contact surface. The

continuous curve displayed on Fig. 4 shows this integrated probability of upstream flame displacement over axial position for a 100% surface contact.

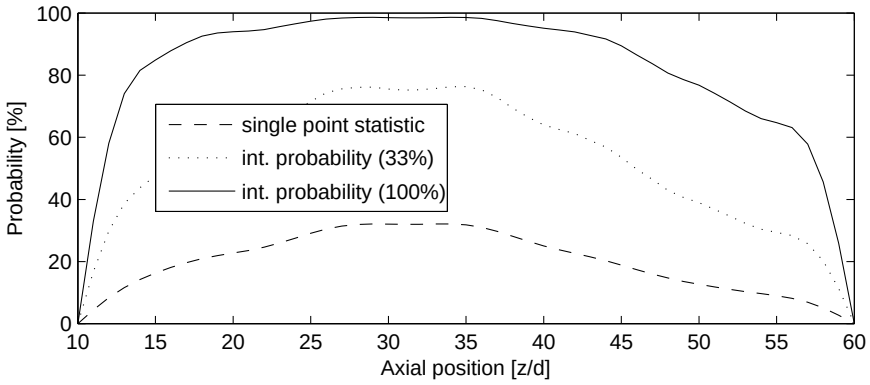

Figure 4: Probability of upstream flame displacement inside the stabilizing region over axial position. Results are shown for a single point and for a contact surface between the flame kernel and the stabilizing ring surface of 33%, respectively of 100% of the stabilizing ring surface.

For an off-axis position, an analytical expression of the number n_{surf} is given by Eq. 9 as a function of the radial position of the kernel center, r_{ker}. Indeed, the number n_{surf} is obtained from the arc length of the tubular zone that is in contact with the flame kernel surface. This tubular zone, $3 < r/d < 4$, is displayed on Fig. 1(d) in light gray, while the representative kernel disk is displayed in dark gray, with a diameter of 7 d, following the experimental observation in [2] of the kernel diameter at transition time to a stable propagating flame.

$$n_{surf}(r_{ker}) = \frac{\pi 7d}{d}\frac{1}{\pi} acos\left(\frac{|r_{ker} - d/2|}{7d}\right) \tag{9}$$

For a radial position of the center of a flame kernel of $r_{ker} = 4\ d$, 33% of the surface of the stabilizing ring is in contact with the kernel surface. The corresponding integrated probability of upstream flame displacement is displayed by the dotted line on Fig. 4.

With respect to the probabilistic convection of the particles after 10 ms, see Fig. 1(c), it is now possible to evaluate the probability that a flame kernel initiated at a given spark location, will encounter upstream flame displacement over its surface after 10 ms. Figure 5(c) shows the probability map of successful ignition, P_{ign}, where it refers to the probability of generating a kernel P_{ker} and of flame stabilization, $P_{up}(z, r_{ker})$, at the location where the kernel has been convected. The probability of ignition is calculated as a product of probabilities.

The predicted probability of ignition is qualitatively consistent with the experimental values, displayed on Fig. 5(a), although numerical differences exist.

A comparison to Fig. 3(b) shows a lower probability for P_{ker} than for P_{ign}, in the downstream region ($z/d > 45$). It indicates that ignited kernels fail to stabilize. The statistical occurrence of lean ignited kernel blow-out events is delayed of an axial distance of 5 d on the jet axis, with respect to the experimental data. In this region, the radial decay is essentially obtained from the modeling used for integrating the probability over the contact surface and the trends are consistent with experimental data.

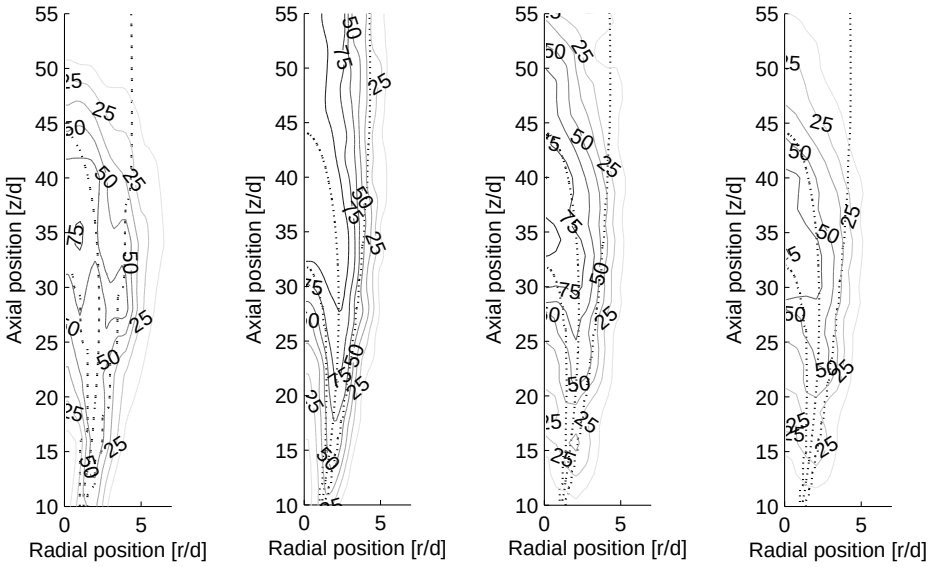

Figure 5: Maps of probability: (a) Experimental results for successful ignition, P_{ign}, in [2], (b) Flammability factor representative of the probability of successful kernel generation, P_{ker}, (c) Probability of successful ignition, P_{ign}, as probability of generating a kernel P_{ker} and of flame stabilization, $P_{up}(z, r_{ker})$. (d) Probability of successful ignition, considering the probability of upstream flame speed higher than a threshold value of $U_{th} = 0.15\ m/s$.

The axial delay in the prediction of the statistical occurrence of blow-out events can be attributed to the definition of the criterion for evaluating the possibility of upstream flame propagation. Indeed, the probability of upstream displacement is calculated as the fraction of points with an upstream flame speed. However, the effective upstream displacement of the flame front requires a flame speed that is strictly positive. Hence, restricting the probability of upstream displacement to the fraction of points with a flame speed higher than a threshold value U_{th}, it is possible to account for this effect.

Figure 5(d) shows the probability map of successful ignition with a threshold speed of $U_{th} = 0.15\ m/s$. This threshold value allows to obtain a probability of successful ignition of 55% on the jet axis at an axial position of $z/d = 45$, as found experimentally. Applying this threshold speed, the probability of ignition is better predicted. In particular, the

radial and axial trends of the statistical occurrence of flame blow-out are better predicted in the downstream region of the jet for $z > 40\ d$, where successfully generated kernels fail to stabilize. A residual probability of possible flame stabilization, less than 25%, is obtained on the jet axis in the range of $50 < z/d < 55$, while this probability should be zero in this domain. The region of high ignition probability is predicted correctly in terms of location and probability level. Hence, the use of a threshold speed for accounting for effective flame upstream displacement seems to be an adequate modeling. However, this approach needs to be validated by further experimental or numerical investigations.

5 CONCLUSION

A LES method for performing statistical analysis of spark ignition events in non-premixed configurations has been developed and validated. The method accounts for the probabilistic kernel generation and convection and for the probability of kernel blow-out at the corresponding location.

The monitoring of Lagrangian fluid particles seeded into the stationary inert flow enables the simultaneous analysis of multiple ignition events. Hence, the modeling allows performing ensemble averaging for prediction of the overall flame ignition probability following a local spark. Statistical analysis of transient phenomena is achieved in a very efficient manner, as the computational cost scales with the cost required for performing standard LES statistics of the inert turbulent configuration.

The comparison of results to experimentally-determined ignition maps demonstrates, that the method is capable of accounting for the probabilistic blow-out of flame kernels and for predicting reasonably well the locations in the jet having high ignition probability.

This method, once improved, is intended to be applied to complex configurations, like gas turbines combustors or IC engines.

6 ACKNOWLEDGMENT

We gratefully acknowledge the financial support of the German Research Foundation within the Graduate School GRK1344 and the CFD-code support by Rolls-Royce Deutschland. We particularly acknowledge the financial support from the European Commission within the FP6 research project TIMECOP-AE.

REFERENCES

[1] E. Mastorakos, Ignition of turbulent non-premixed flames, Progress in Energy and Combustion Science 35 (2009) 57–97.

[2] S. F. Ahmed, E. Mastorakos, Spark ignition of lifted turbulent jet flames, Combustion and Flame 146 (2006) 215–231.

[3] G. Lacaze, E. Richardson, T. Poinsot, Large eddy simulation of spark ignition in a turbulent methane jet, Combustion and Flame 156 (2009) 1993–2009.

[4] A. D. Birch, D. R. Brown, M. Godson, Ignition probability in turbulent mixing flows, Proceedings of the 18th Combustion Symposium (1981) 1775–1780.

[5] M. Smith, A. Birch, D. Brown, M. Fairweather, Studies of ignition and flame propagation in turbulent jets of natural gas, propane and a gas with a high hydrogen content, Proceedings of the 21st Combustion Symposium (1986) 1403–1408.

[6] S. F. Ahmed, R. Balachandran, E. Mastorakos, Measurements of ignition probability in turbulent non-premixed counterflow flames, Proceedings of the Combustion Institute 31 (2007) 1507–1513.

[7] S. F. Ahmed, R. Balachandran, T. Marchione, E. Mastorakos, Spark ignition of turbulent non-premixed bluff-body flames, Combustion and Flame 151 (2007) 366–385.

[8] J. Janicka, A. Sadiki, Large eddy simulation of turbulent combustion systems, Proceedings of the Combustion Institute 30 (2005) 537–547.

[9] M. Boileau, G. Staffelbach, B. Cuenot, T. Poinsot, LES of an ignition sequence in a gas turbine engine, Combustion and Flame 154 (2008) 2–22.

[10] A. Triantafyllidis, E. Mastorakos, R. Eggels, Large Eddy Simulations of forced ignition of a non-premixed bluff-body methane flame with Conditional Moment Closure, Combustion and Flame 156 (2009) 2328–2345.

[11] V. Subramanian, P. Domingo, and L. Vervisch. Large eddy simulation of forced ignition of an annular bluff-body burner, Combustion and Flame 157 (2010) 579–601.

[12] O. Vermorel, S. Richard, O. Colin, C. Angelberger, A. Benkenida, D. Veynante, Towards the understanding of cyclic variability in a spark ignited engine using multi-cycle les, Combustion and Flame 156 (8) (2009) 1525 – 1541.

[13] E. Richardson, Ignition modelling for turbulent non-premixed flow, Ph.D. thesis, Cambridge University (2007).

[14] M. Germano, U. Piomelli, P. Moin, W. Cabot, A dynamic subgrid-scale eddy viscosity model, Physics of Fluids A 3 (7) (1991) 1760–1765.

[15] A. Yoshizawa, Statistical theory for compressible turbulent shear flows, with the application to subgrid modeling, Physics of Fluids 29 (7) (1986) 2152–2164.

[16] A. Pocheau, Front propagation in a turbulent medium, Europhysics Letters 20 (1992) 401.

[17] H. Im, Study of turbulent premixed flame propagation using laminar flamelet model, Center for Turbulence Research, Annual Research Briefs (1995) 347–360.

[18] M. Düsing, A. Sadiki, J. Janicka, Towards a classification of models for the numerical simulation of premixed combustion based on a generalized regime diagram, Combustion Theory and Modelling 9 (2005) 1–28.

[19] M. Metghalchi, J. C. Keck, Burning velocities of mixtures of air with methanol, isooctane, and indolene at high pressure and temperature, Combustion and Flame 48 (2) (1982) 191–210.

[20] G. P. Smith, D. M. Golden, M. Frenklach, N. W. Moriarty, B. Eiteneer, M. Goldenberg, C. T. Bowman, R. K. Hanson, S. Song, W. C. Gardiner, V. V. Lissianski, Z. Qin. www.me.berkeley.edu/gri_mech.

[21] C. Richards, W. Pitts, Global density effects on the self-preservation behaviour of turbulent free jets, Journal of Fluid Mechanics 254 (1993) 417–435.